Gust and Ground Loads Integration for Aircraft Landing Loads Prediction

A. Castrichini[1], J.E. Cooper[2]
University of Bristol, Bristol, BS8 1TH, United Kingdom

T. Benoit[3],Y. Lemmens[4]
Siemens PLM Software, Leuven, Interleuvenlaan 68 B-3001, Belgium

A methodology is described to couple unsteady aerodynamic loads with flexible bodies in multibody simulations. A representative civil jet aircraft aeroelastic model is used to evaluate the structural loads due to the combination of gust and ground loads.The implementation of unsteady aerodynamic loads is validated by comparing the results for the wing root bending moment and tip displacement with Nastran transient aeroelastic analyses for a series of gust lengths of a linear free-free aircraft model. The main objective of the paper is to prove that with the implementation of a time domain formulation for the unsteady aerodynamic loads, a multibody simulation can be used to predict the aircraft aeroelastic loads that are comparable with traditional FEM-based methods. However, the use of a multibody simulation software offers the simulations to other manoeuvres such as landings and the use of non-linear and active structures.

Nomenclature

Symbols

A	=	Rotation matrix
b_l	=	Aerodynamic lag-pole
c	=	Mean chord
C	=	Constraint forces
D	=	Damping matrix
H	=	Gust gradient
F_{Aero}	=	Aerodynamic forces vector
k	=	Reduced frequency
K	=	Stiffness matrix
L_g	=	Gust length
M	=	Mass matrix
$MAST$	=	Moment Axial Shear Torque loads
q_{dyn}	=	Dynamic pressure
V	=	True air speed
w	=	Gust vector
w_g	=	Gust velocity
w_{g0}	=	Peak of the gust velocity
w_{ref}	=	Reference gust velocity
x_0	=	Gust origin position
x_j	=	jth panel's control node position
α	=	Angle of attack
γ_j	=	jth panel's dihedral angle
δ	=	Aerodynamic control surfaces vector
Λ	=	Hinge orientation angle
ξ	=	Generalized coordinates vector
ξ_h	=	Modal coordinate
λ	=	Lagrange multiplier

[1] PhD Student, Dept. of Aerospace Engineering
[2] Airbus Royal Academy of Engineering Sir George White Professor of Aerospace Engineering, AFAIAA
[3]Research Engineer, Aerospace Competence Centre
[4] Project Leader RTD, Aerospace Competence Centre

q_f	=	Modal coordinates	Φ	=	Modal base
Q_0	=	Generalized aerodynamic force matrices	Ψ	=	Body reference rotation
Q_e	=	External forces	*Superscript*		
Q_{i0}	=	Coefficient matrices of RFA	$\hat{}$	=	Nondimensional quantities
Q_v	=	Quadratic velocity forces	$\cdot$	=	Differentiation with respect to time
r	=	Point global position	$\tilde{}$	=	Fourier transform
R	=	Body reference translation	$\bar{}$	=	Generalized variable
R_l	=	Aerodynamic states vector	*Subscript*		
s	=	Span local coordinate	0	=	Initial value
u	=	Point local position			

I. Introduction

Aircraft load prediction is used to identify the maximum structural loads in an aircraft during flight and ground manoeuvres and during gusts. This papers focuses on the extension of the generic multibody simulation software LMS Virtual.Lab Motion with aerodynamic modelling capabilities to support a more reliable prediction of aircraft flight and ground loads. The motivation to use multibody simulation software was to enable the inclusion of non-linear or active systems.

Traditionally, the doublet lattice method[1,2] (DLM), often corrected with CFD or wind tunnel test results, coupled with structural FEM models are used to predict aerodynamic aircraft loads. These linear aeroelastic analyses are typically solved in the frequency domain. However, to include non-linear or active systems, such as a landing gear for ground manoeuvres, or control surface attachments, a multibody simulation is more suitable.

Multibody simulations (MBS) represent a valuable tool for aircraft loads assessment and structure design. It is a standard practice, within the aeronautical industry, to rely on MBS for the design of complex nonlinear systems such as high-lift devices' or aerodynamic control surfaces' mechanisms, landing gears, helicopter's rotors and blades. Furthermore MBS are a state of art tool for the evaluation of aircraft ground loads due to taxing, landing, turning and take-off manoeuvres.

In the last years there was a growing interest within the academic and industrial community in the use of multibody software for aeroelastic applications as well. Such kind of approach was made attractive by the possibility of performing nonlinear and multidisciplinary analyses allowing the combination of nonlinear structural dynamics, aerodynamics as well as nonlinear controls or actuation systems (e.g. landing gears' oleo-damping system, fuel plant, engines trust model...) where required. Multibody simulations are particularly suitable for aeroelastic application when large rigid body motions need to be taken into account, as for the simulation of aircraft manoeuvres or morphing

aircraft shape changing, as well as for the simulation of complex manoeuvres like a landing where aerodynamic and ground loads combination is essential for a reliable analysis. Another significant advantage is given by the direct coupling of aeroelastic and nonlinear flight mechanics equations of motion. Such coupling is, in general, not supported by commercial aeroelastic finite element codes, such as Nastran, which consider only linear flight mechanics for loads and stability analyses. Significant efforts has been made trying generate aircraft models combining flight dynamics and airframe structural flexibility[3-13] however this is still not a common practice for industrial applications which has found MBS to be a more straight forward approach.

Despite the need to produce accurate model, unsteady aerodynamic forces, accounting for the body flexibility effects are not supported by commercial multibody software and many efforts have been made previously in order to implement aeroelastic loads in multibody dynamic simulations. Several authors[14-17] have proposed a quasi-steady approach by means of strip-theory. The wing was discretised, along the spanwise direction, using rigid sections connected through springs elements defining the bending and torsional wing stiffness. The structural sections were able to undergo finite relative rotations with respect to each other allowing highly nonlinear wing deflections. The aerodynamic forces were defined as a function of the local angle of attack of each section by using a suitable set of aerodynamic coefficients from a predefined aerodynamic database. Although this approach allows the coupling of flight dynamics and aeroelastic equations, the standard strip theory method does not account neither for unsteady aerodynamic effects nor for the aerodynamic coupling between each strips. Another approach, proposed by Spieck and Krüger[18-20] consisted in the definition of a generalised aerodynamic database built using CFD data. A flexible linear structure was considered and the aerodynamic forces were formulated in a quasi-steady fashion by retrieving aerodynamic stiffness and damping coefficients, associated to each structural mode, by means of CFD calculations. Although such approach does not allow to account for structural nonlinearities, being the aircraft flexibility defined using Rayleigh-Ritz methods, it leads to a significant improvement over the aerodynamic modelling with respect the strip theory. Other authors exploited the advantages of using multibody solver to investigate the aeroelastic effects due to the change of shape of a morphing aircraft by using a quasi-steady CFD aerodynamic database[21] or by a tight coupling with an external vortex lattice method aerodynamic model[22-24]. A more advanced approach was proposed by Cavagna et Al.[25,26] who directly coupled an aircraft multibody model with an external CFD code for accurate loads and manoeuvres calculations.

However, gusts with a short length and impulse loads, such as during a landing, result in a high frequency response of the aircraft that requires also take into account the unsteady effects of the aerodynamic forces. Because the multibody simulation is a time-domain simulation and the unsteady aerodynamics is modelled with the doublet lattice method, which is a formulated in the frequency domain, an approximation of the latter was required to allow such methodology in a time domain solution.

The implementation has been validated by comparing the results of the multibody solution with the Nastran aeroelastic analyses. The multibody simulations used as input the same aerodynamic matrices from the Nastran aeroelastic analyses.

II.The Equation of Motion of Multibody Analysis with Deformable Components

Industrial and technological systems can be represented as collections of bodies connected by joints, subjected to mutual and external forces. In order to analyse the dynamic behaviour of these systems, it is necessary to use multibody simulation tools, which, differently from the classic linear finite element codes, allow to correctly model the highly non-linear effects due to the large body rotations.

Originally the multibody codes could deal only with rigid bodies, whose motion could be described by using 6 generalized coordinates, but in many applications a large number of elastic coordinates have to be taken into account in order to accurately describe the body dynamic response. Many formulations have been proposed in literature to include the flexibility of a subcomponent in a multibody analysis, such as the floating frame of reference technique (FFR), the finite segment method, the finite element incremental method and so on[27,28]. The floating frame of reference, is the formulation which has found the most widespread application and implementation in the commercial multibody packages, such as LMS Virtual.Lab Motion. When the FFR formulation is used, the configuration of each deformable body in the multibody system is identified by using two sets of coordinates[27,28]:

- The reference coordinates which define the location, R^i and orientation, Ψ^i, of a generic i^{th} body's reference.
- The elastic coordinates describe the body local deformation, u_a^i, with respect to the body reference and are introduced by using classical approximation techniques such as Rayleigh-Ritz methods.

Figure 1 shows the global position, r^i of an arbitrary point of the generic i^{th} body that can be expressed as

$$r^i = R^i + A^i(u_0^i + u_a^i) \tag{1}$$

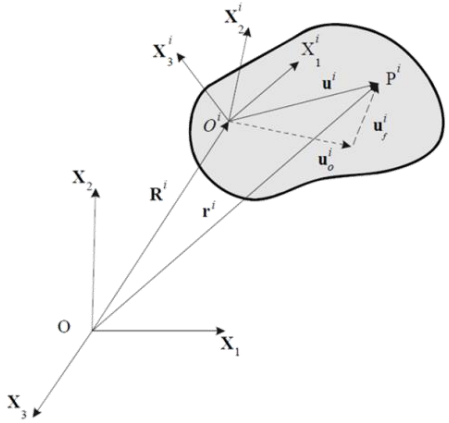

Figure 1. Floating Frame Of Reference[27]

where A^i is the transformation matrix that defines the orientation of the body reference $[X_1^i, X_2^i, X_3^i]$ with respect to the global reference $[X_1, X_2, X_3]$ and it can be expressed in terms of Euler parameters, Euler angles or Bryant angles; u_0^i is the undeformedposition of the point in the body reference system.

In particular the nodal elastic displacement u_a^i, are described as a linear combination of eigenmodes, Φ_{ah}^i,according a set of proper modal participation factors (MPF), ξ_h^i, as follow

$$u_a^i(x,t) = \sum_{n=1}^{N_{Modes}} \Phi_{ah}^i(x)\, \xi_h^i(t) \tag{2}$$

This means that, despite the multibody code allowing the modelling of nonlinear finite translations and rotations for the body reference coordinates, the elastic coordinates, with the related modal shapes, can only describe small and linear deformations. The selected shape functions have to satisfy the kinematic constraints imposed on the boundaries of the related deformable body due to the connection chain between the different subcomponents; therefore Craig-Bampton[29] mode sets are generally defined to take attachment effects into account.

The origin of the floating reference frame does not have to be rigidly attached to a material point on the deformable body, but it is required that there is no rigid body motion between the body and its coordinate system. This restriction means that the rigid body modes have to be removed from the modal basis used to describe the body deformation. The selection of the body reference is a key parameter for the correct formulation of the problem. For rigid body dynamics it is common to use centroidal body coordinates in order to decouple the inertial properties of rotational and translational degrees of freedom. However, the floating frame of reference formulation does not necessary lead to a

separation between the rigid body motions and the elastic deformations, which may be coupled by the inertial properties of the body. This coupling strongly depends upon the choice of the floating frame of reference with respect to which the modal shapes are defined. A weak inertial coupling could be achieved by using a mean-axis-frame, which requires using the eigenvectors of free-free structures[30]. With respect to the mean-axis-frame, the flexible modes do not induce any motion of the body centre of gravity, thus allowing minimization of the kinetic energy related to the flexible modes, leading to a weak coupling between the reference motion and the elastic deformation[31].

The mean-axis-frame enlarges also the applicability of the linearised equations for the flexible degrees of freedom since it is the reference with respect to which the deformations of the flexible body are minimized.The nonlinear dynamics equations of motion for a system of interconnected flexible and rigid bodies are formulated as

$$\bar{M}^i\ddot{\xi}^i + \bar{D}^i\dot{\xi}^i + \bar{K}^i\xi^i + \bar{C}^T_{\xi^i}\lambda = \bar{Q}^i_v + \bar{Q}^i_e \qquad i = 1, \dots, N_{bodies}$$

$$\begin{bmatrix} \bar{M}^i_{RR} & \bar{M}^i_{R\Psi} & \bar{M}^i_{Rh} \\ \bar{M}^i_{\Psi R} & \bar{M}^i_{\psi\psi} & \bar{M}^i_{\Psi h} \\ \bar{M}^i_{hR} & \bar{M}^i_{h\Psi} & \bar{M}^i_{hh} \end{bmatrix} \begin{Bmatrix} \ddot{R}^i \\ \ddot{\Psi}^i \\ \ddot{\xi}^i_h \end{Bmatrix} + \begin{bmatrix} 0 & 0 & 0 \\ 0 & 0 & 0 \\ 0 & 0 & \bar{D}^i_{hh} \end{bmatrix} \begin{Bmatrix} \dot{R}^i \\ \dot{\Psi}^i \\ \dot{\xi}^i_h \end{Bmatrix} + \begin{bmatrix} 0 & 0 & 0 \\ 0 & 0 & 0 \\ 0 & 0 & \bar{K}^i_{hh} \end{bmatrix} \begin{Bmatrix} R^i \\ \Psi^i \\ \xi^i_h \end{Bmatrix} + \tag{3}$$

$$\begin{Bmatrix} \bar{C}^T_{R^i} \\ \bar{C}^T_{\Psi^i} \\ \bar{C}^T_{\xi^i_h} \end{Bmatrix} \lambda = \begin{Bmatrix} \bar{Q}^i_{vR} \\ \bar{Q}^i_{v\Psi} \\ \bar{Q}^i_{v\xi_h} \end{Bmatrix} + \begin{Bmatrix} \bar{Q}^i_{eR} \\ \bar{Q}^i_{e\Psi} \\ \bar{Q}^i_{e\xi_h} \end{Bmatrix} i = 1, \dots, N_{bodies}$$

where ξ is the vector of the generalized coordinates of the body which includes the rigid body translations $\{R_1, R_2, R_3\}$ and rotations $\{\Psi_1, \Psi_2, \Psi_3\}$ and the modal elastic coordinates ξ_h (h =1, ...,N_{Modes}) related to the linear flexible bodies, $\bar{M}$, $\bar{D}$, $\bar{K}$ are the generalized mass, damping and stiffness matrices respectively, $C^T$is the constraint forces vector and λ the related Lagrange multiplier, $Q_v$are the quadratic velocity forces (Coriolis and centrifugal terms) and $Q_e$are the external forces.

III.Internal Loads Evaluation in a Multibody Analysis

A methodology to evaluate the integrated internal loads of a flexible body in dynamic multibody analyses is introduced here.Such loads are due to the redistribution within the structure of the applied external loads (e.g. aerodynamic, inertial, ground loads...). An accurate evaluation is required since these loads are used both in the preliminary phase of an aircraft, during which a great number of loads scenarios have to be evaluated in order to correctly size the

structure of the aircraft, but also during the in-service life of the aircraft in order to evaluate the potential failure due to a ground or flight incidents.

These internal loads are not only function of the magnitude of the external loads, but also of the their distribution over the structure.

In aeronautical applications, where slender bodies, such as wings and fuselage, are considered, it is fundamental to evaluate the trends of the internal bending Moment, Axial and Shear forces and Torque moments (MAST) along with the structural component of interest with respect to a local reference system[32]. The external loads distribution, Fig. 2(a), is assumed as known when internal MAST loads need to be evaluated. The structure is cut virtually at the section of interest and divided in two subsections. The free body equilibrium is then performed to evaluate the internal interface forces and moments balancing the external loads applied to the substructure, as shown in Fig. 2(b).

(a) Aircraft distributed loads[32] (b) Integration of the loads a specific section[32]

Figure 2. Integral Internal Loads Evaluation Process

In order to calculate such integrated structural loads, it is required to recover the nodal loads distribution during a dynamic event. Several methods can be used for the evaluation of the internal forces distribution such as the modal displacement method, the direct summation forces or the modal acceleration method[33].

For the modal displacement method the modal internal structural loads are evaluated through the combination of the modal external, damping and inertial loads. The nodal loads distribution is retrieved by combining the modal participation factors ξ_h with a respective set of modal internal loads as

$$K_{aa}u_a = \Phi_{ah}\overline{K}_{hh}\xi_h = \Phi_{ah}\left(\bar{Q}_e - \overline{M}_{hh}\ddot{\xi}_h - D_{hh}\dot{\xi}_h\right) \tag{4}$$

This method works particularly well when the applied loads are quite regular, in terms of spatial distribution, as generally the aerodynamic loads are. A smooth aerodynamic load distribution is mainly orthogonal to the higher frequency modes, which are characterised by a significant spatial waviness, therefore a relative small number of modal loads should be enough to allow the converge of this method and to accurately evaluate the integrated structural loads.

However this method may suffer of local and global convergence problems in the presence of concentrated loads (such as the ones exchanged at the wing/landing gear or wing/engine attachments), irregular loads distribution, significant lumped masses and massless points with applied loads, whose local displacement cannot be captured by any normal mode. Such convergence problems arise since the spatial loads distribution is recovered combining modal contributions. The normal modes are by definition evaluated for an unloaded structure and therefore they are not influenced by the applied loads (at least for a linear problem), leading the selected modal base not suitable to represent every generic loads distribution. Obviously such a method is particularly suitable when generalised aerodynamic forces are used as this is directly defined on the same modal base used for the analysis and also the doublet lattice method.

Once the internal structural loads distribution is known, the integrated MAST loads can be retrieved by the direct summation of the nodal contributions over the structural component of interest.

The modal displacement method was selected for the structural loads recovery, this being the only possible approach due to the generalised formulation of the aerodynamic loads. In the case of a concentrated load the convergence of this method can be enhanced through the use of a proper set of shape functions as demonstrated in the following section.

Figure 3 shows the algorithm used for the internal loads evaluation:

- A Nastran modal analysis is performed to evaluate the normal modes used to define the flexible properties of a generic i^{th} flexible body.
- A dynamic analysis is performed and the multibody solver provides the modal participation factors, at each time step $\xi_h^i(t)$.
- The modal loads, at a specified structural section $\bar{s}$ and for a specific h^{th} mode, are given by the integration of the internal forces in $\bar{s}$, when the structure is statically deformed as the h^{th}mode. These modal loads are evaluated by defining several static solutions, where each mode shape is imposed to the structure as a prescribed deformation by using the Nastran SPC cards (single point constraints). The finite element code solves for each modal shape Φ_{ah}^i the static solution and provides as output the constraint forces on each node which are then integrated providing the modal MAST loads as

$$\overline{MAST}_{ah}^i(\bar{s}) = \int_{\bar{s}} K_{aa}^i \Phi_{ah}^i \tag{5}$$

Where K_{aa}^{i} is the structural stiffness matrix and $K_{aa}^{i}\Phi_{ah}^{i}$ represent the nodal constraint forces distribution. The structure is virtually cut in two separate portions at $\bar{s}$ and the free body equilibrium is used to calculate the internal integral loads on the section of interest. The free body equilibrium is automatically performed by Nastran with the monitor point card, MONPNT3, which integrates the loads applied on a specific set of nodes and elements with respect a selected reference system.

- MPF and modal loads are then combined as

$$MAST^{i}(\bar{s},t) = \sum_{h=1}^{N_{Modes}} \overline{MAST}_{ah}^{i}(\bar{s})\,\xi_{h}^{i}(t) \tag{6}$$

providing the time variation of the integrated loads at $\bar{s}$.

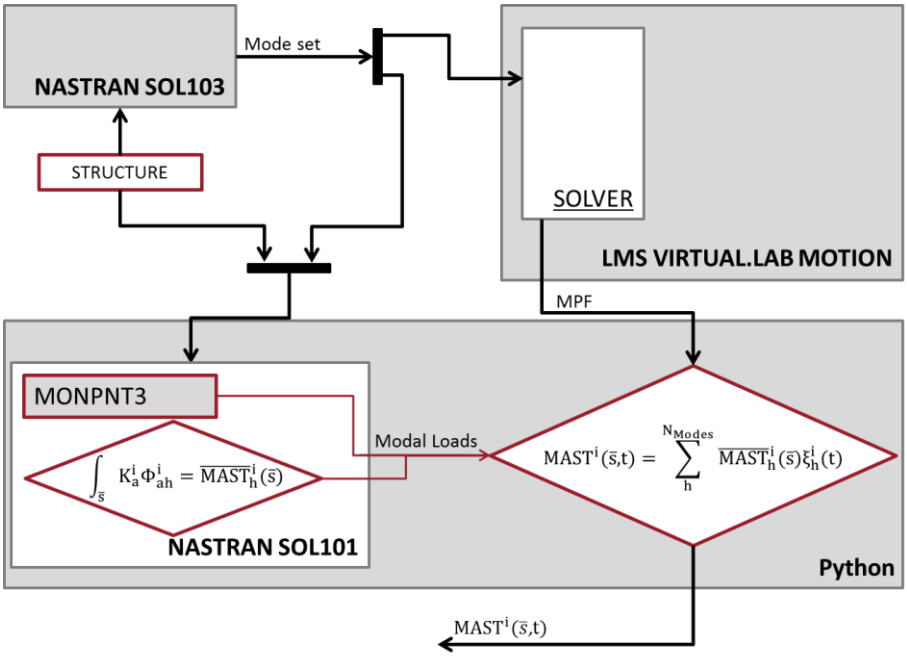

Figure 3.Integral Internal Loads Evaluation Process

IV.Aerodynamic Model

The doublet lattice method[1,2] represents a standard and consolidated tool within the aeronautical industry and it was employed to model the aerodynamic forces which, in the frequency domain, are defined as

$$F_{Aero} = q_{dyn}[Q\tilde{\xi} + Q_x\tilde{\delta} + Q_g\tilde{w}] \tag{7}$$

where $Q_{(N_{Modes}+6\ X\ N_{Modes}+6)}$, $Q_{x(N_{Modes}+6\ X\ N_{ControlSurf})}$ and $Q_{g(N_{Modes}+6\ X\ N_{Panels})}$ are respectively the generalized aerodynamic forces matrices related to the Fourier transform of the generalized coordinates $\tilde{\xi}$, control surfaces vector $\tilde{\delta}$ and gust vector $\tilde{w}$.

The aerodynamic forces due to the control surfaces deflection were evaluated by means of transpiration boundary conditions, i.e. by applying a local variation of the downwash velocity on the related aerodynamic panels without actually rotate them.

The gust vector defines the downwash on a generic aerodynamic panel *j* due to the gust such that

$$w_j = b_j(y)\cos\gamma_j \frac{w_{g0}}{2V}\left(1 - \cos\left(\frac{2\pi V}{L_g}\left(t - \frac{x_0 - x_j}{V}\right)\right)\right) \tag{8}$$

Where $b_j(y)$ is the gust span shape function, γ_j is the dihedral angle of the j^{th} panel, $x_0 - x_j$ is the distance of the j^{th} panel with respect the gust origin, L_g is the gust length (twice the gust gradient *H*), V is the true air speed and w_{g0} peak gust velocity. The latter defined (in m) as

$$w_{g0} = w_{ref}\left(\frac{H}{106.17}\right)^{\frac{1}{6}} \tag{9}$$

The aerodynamic matrices Q, Q_x, Q_g were computed for a limited number of reduced frequencies $\left(k = \frac{\omega c}{2V}\right)$ and at a givenMach number M.

In order to allow for simulation in the time domain, the aerodynamic matrices were approximated, in the frequency domain, using the rational fraction approximation method proposed by Roger[34].

Following some manipulation, the aerodynamic loads can be formulated in the time domain as

$$\begin{aligned} F_{Aero} = q_{dyn}\Bigg\{&\left[Q_0\xi + \frac{c}{2V}Q_1\dot{\xi} + \left(\frac{c}{2V}\right)^2 Q_2\ddot{\xi}\right] + \left[Q_{x0}\delta + \frac{c}{2V}Q_{x1}\dot{\delta} + \left(\frac{c}{2V}\right)^2 Q_{x2}\ddot{\delta}\right] \\ &+ \left[Q_{g0}w + \frac{c}{2V}Q_{g1}\dot{w} + \left(\frac{c}{2V}\right)^2 Q_{g2}\ddot{w}\right] + \sum_{l=1}^{N_{Poles}} R_l\Bigg\} \end{aligned} \tag{10}$$

where R_l is the generic aerodynamic state vector related to the generic lag-pole $\left(b_l = \frac{k_{max}}{l}\right)$. These extra states allowed the modeling of the unsteady response of the aerodynamics by taking into account of the delay of the aerodynamic

forces with respect to the structural deformations. These aerodynamic states were evaluated through the set of dynamic equations

$$\dot{R}_l = -b_l \frac{2V}{c} IR_l + Q_{2+l}\dot{\xi} + Q_{x2+l}\dot{\delta} + Q_{g2+l}\dot{w} \qquad l = 1, \dots, N_{Poles} \tag{11}$$

and these equations were solved using the LMS Virtual.Lab Motion solver together with the equations of motion.

Note that the gust is not modelled as a single scalar value, but as vector of gusts defined for each aerodynamic panel. Each component of the gust vector w_j is delayed in time in function of the position of the related panel with respect the origin of the gust. Although this approach leads to bigger aerodynamic matrices matrices ($Q_g$is ($\mathrm{N_{Modes}} +$ 6 X N_{Panels}), it does enable a more accurate approximation of the aerodynamic gust terms. The modelling of the delay directly in the time domain, and not in the frequency domain, has prevented the typical spiral trend[35-38] which in general affects the gust terms and that is poorly approximated when a restricted number of extra aerodynamic poles are used. In the a following Section it will be shown how this reflects in an almost perfect match between the Nastran gust analysis results and the approximated gust analysis in the time domain.

Furthermore, having defined a dedicated downwash vector for each panel enables also the straight forward modelling of non uniform spanwise gust by simply defining an arbitrary function $b_j(y)$ which scales the intensity of the gust vector in function of the spanwise position of the aerodynamic panel.

The gust is assumed to travel along the roll aircraft axis. The panels' dihedral angles γ_j are defined as the angles between the gust vector and the normal vector to the Doublet Lattice surface. The gust vector can be defined either along the global z or y axes for vertical and gusts respectively. Any intermediate gust direction can be defined by a suitable linear superposition of vertical and lateral gust components.

Although the doublet lattice method is an industrial standard approach for the evaluation of aeroelastic loads and stability, it is not suitable tool for the modelling of rigid aircraft flight dynamics. Given the assumption of small perturbation of a mean uniform flow, only the aerodynamic loads due to small elastic deformations and small rigid body motions with respect an undeformed reference conditions are accounted. The nonlinear effects introduced by finite aircraft rotations are neglected, while the aerodynamic coupling between the rigid degrees of freedom are not accounted or underestimated, apart from the pitch and plunge motions. Therefore the typical longitudinal and lateral flight dynamics modes are not conveniently represented. Only the short period mode, which is in general excited by the gusts, is accounted for by the doublet lattice method.

It is important to point out that the focus of this paper was not the generation of a coupled flight mechanics aeroelastic model, but the analysis of the aircraft loads during a landing manoeuvre.

Aerodynamic loads were introduced in the multibody software to allow aeroelastic trim and gust analyses when nonlinear structural elements, such as landing gears, are defined. The same level of accuracy of the standard Nastran formulation was considered to be satisfactory for the aerodynamic loads definition

Therefore the double lattice method was employed to define the rigid body aerodynamic forces as well. The free-free structural modes were calculated using the Givens method in order to have rigid body modes that represented translations and rotations around the centre of gravity of the aircraft. These modes were scaled to involve unit translations and rotations so that the aerodynamic generalized forces related to the rigid body modes were related with the rigid body generalized coordinates of the LMS Virtual.Lab Motion model (i.e. $\{\xi_1, \xi_2, \xi_3, \xi_4, \xi_5, \xi_6\} \approx \{R_1, R_2, R_3, \Psi_1, \Psi_2, \Psi_3\}$). In particular the rigid body angles represent the roll, pitch and yaw angle respectively.

It was found that the rigid body forces were particularly sensitive to the stiffness and damping terms of the related aerodynamic forces, a small error on their evaluation could lead the solution to diverge after the gust event. A solution was found by defining a hybrid rational function approximation of the aerodynamic matrix Q_{hh} as shown in Fig. 4:

- A quasi-steady formulation for the rigid body modes columns, with a maximum reduced frequency of k_{max} =0.01 and no extra aerodynamic poles so that

$$Q[i,j](k,M) \approx Q_0 + ikQ_1 + (ik)^2 Q_2 \quad (j = 1, \dots, 6) \tag{12}$$

- An unsteady formulation for the flexible modes terms, with a maximum reduced frequency of k_{max}=1. and 5 extra aerodynamic poles such that

$$Q[i,j](k,M) \approx Q_0 + ikQ_1 + (ik)^2 Q_2 + \sum_{l=1}^{5} \frac{ik}{ik + b_l} Q_{2+l} \quad (j = 7, \dots, N_{Modes} + 6) \tag{13}$$

This approach was acceptable due to the low frequency range of the rigid body degrees of freedom and ensured a more accurate modeling of their related aerodynamic stiffness and damping forces terms.

The final formulation of the equation of motion of the multibody assembly is therefore given by

$$\bar{M}^i \ddot{\xi}^i + \bar{D}^i \dot{\xi}^i + \bar{K}^i \xi^i + \bar{C}_{\xi^i}^T \lambda = \bar{Q}_v^i + \bar{Q}_e^i + \bar{F}_{Aero}^i \qquad i = 1, \dots, N_{bodies} \tag{14}$$

$$\begin{bmatrix} \bar{M}^i_{RR} & \bar{M}^i_{R\Psi} & \bar{M}^i_{Rh} \\ \bar{M}^i_{\Psi R} & \bar{M}^i_{\Psi\Psi} & \bar{M}^i_{\Psi h} \\ \bar{M}^i_{hR} & \bar{M}^i_{h\Psi} & \bar{M}^i_{hh} \end{bmatrix} \begin{Bmatrix} \ddot{R}^i \\ \ddot{\Psi}^i \\ \ddot{\xi}^i_h \end{Bmatrix} + \begin{bmatrix} 0 & 0 & 0 \\ 0 & 0 & 0 \\ 0 & 0 & \bar{D}^i_{hh} \end{bmatrix} \begin{Bmatrix} \dot{R}^i \\ \dot{\Psi}^i \\ \dot{\xi}^i_h \end{Bmatrix} + \begin{bmatrix} 0 & 0 & 0 \\ 0 & 0 & 0 \\ 0 & 0 & \bar{K}^i_{hh} \end{bmatrix} \begin{Bmatrix} R^i \\ \Psi^i \\ \xi^i_h \end{Bmatrix} +$$
$$\begin{Bmatrix} \bar{C}^T_{R^i} \\ \bar{C}^T_{\Psi^i} \\ \bar{C}^T_{\xi^i_h} \end{Bmatrix} \lambda = \begin{Bmatrix} \bar{Q}^i_{vR} \\ \bar{Q}^i_{v\Psi} \\ \bar{Q}^i_{v\xi_h} \end{Bmatrix} + \begin{Bmatrix} \bar{Q}^i_{eR} \\ \bar{Q}^i_{e\Psi} \\ \bar{Q}^i_{e\xi_h} \end{Bmatrix} + \begin{Bmatrix} \bar{F}^i_{AeroR} \\ \bar{F}^i_{Aero\Psi} \\ \bar{F}^i_{Aero\xi_h} \end{Bmatrix} \quad i = 1, \dots, N_{bodies}$$

where the aerodynamic forces are evaluated as in Eq. (10). Equations (14) are also coupled with Eqs. (11) describing the unsteady aerodynamic effects.

A further modelling effort is required to allow the simulation of nonlinear flight manoeuvres. The author envisages a hybrid approach by replacing the first 6X6 submatrices of the aeroelastic stiffness and damping matrices, respectively $Q_0^{\xi,\delta}$ and $Q_1^{\xi,\delta}$, using more reliable CFD analyses or wind tunnel test, where available, or by correcting the doublet lattice aerodynamics. In this way a more accurate definition of the aerodynamic forces due the rigid body motion would allow a better representation of the nonlinear flight dynamics effects while the aeroelastic forces due to the local elastic deformation would be still modelled by means of the doublet lattice method.

However such aerodynamic modelling improvement was far beyond the scope of this work and future research activities will tackle these aspects.

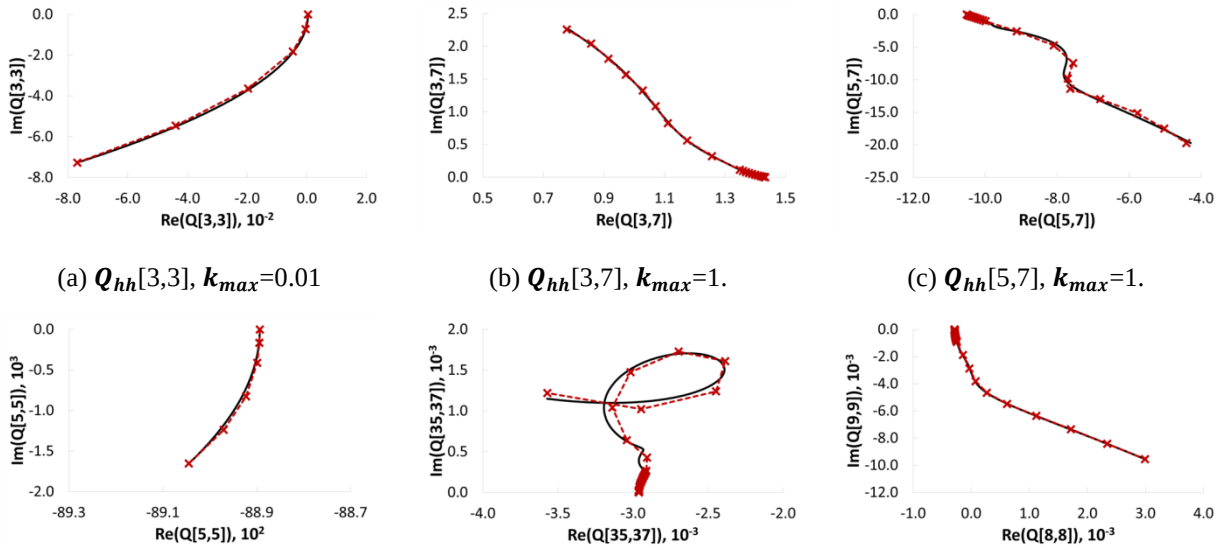

(a) $\boldsymbol{Q_{hh}}$[3,3], $\boldsymbol{k_{max}}$=0.01 (b) $\boldsymbol{Q_{hh}}$[3,7], $\boldsymbol{k_{max}}$=1. (c) $\boldsymbol{Q_{hh}}$[5,7], $\boldsymbol{k_{max}}$=1.

(d) $\boldsymbol{Q_{hh}}$[5,5], $\boldsymbol{k_{max}}$=0.01 (e) $\boldsymbol{Q_{hh}}$[35,37], $\boldsymbol{k_{max}}$=1. (f) $\boldsymbol{Q_{hh}}$[9,9], $\boldsymbol{k_{max}}$=1.

Figure 4. Generalized Hybrid Roger's RFA of the Generalized Aerodynamic Matrix $\boldsymbol{Q_{hh}}$ (-✱-: Nastran; ——: RFA)

V.User Defined Force Element

A description of the unsteady aerodynamic forces implementation within the multibody solver is now considered. The aerodynamic loads are introduced in the multibody code by using a User Defined Force element, UDF, which is given by a Fortran77 routine that can be written by the user and allows the definition of a customised force to be applied on the body during the dynamic analysis. The logical structure of the UDF, shown in Fig.5, is the following:

- A pre-process step consisting in the evaluation of the flexible body modes describing the flexible properties of the airframe. The aerodynamic matrices are also extracted from Nastran and the RFA is performed in order to allow their use in a time domain simulation.
- At the first time step the code reads and stores in the memory the aeroelastic matrices resulting from the RFA.
- At each time step aeroelastic matrices and generalised displacements, including the rigid body motion and the elastic deformations, are combined leading to a set of generalised forces.
- The generalized aerodynamic forces are then applied on the related generalized coordinates of the body of interest.
- Aeroeservoelastic simulations are supported by running the multibody solver in parallel with Matlab Simulink. Aircraft rigid body displacements and velocities define the inputs for the automatic controls evaluating the control surfaces deflections required for a prescribed manoeuvre. The control surfaces deflections are sent from Simulink back to the UDF which generates the related aerodynamic forces to be applied on the body.
- The UDF defines also the aerodynamic states equation to be solved by the multibody solver as well as the external gust profile input.
- The final outcome of the simulation are the modal participation factors which are used as input for the structural internal loads calculations as described in Eq. (6).

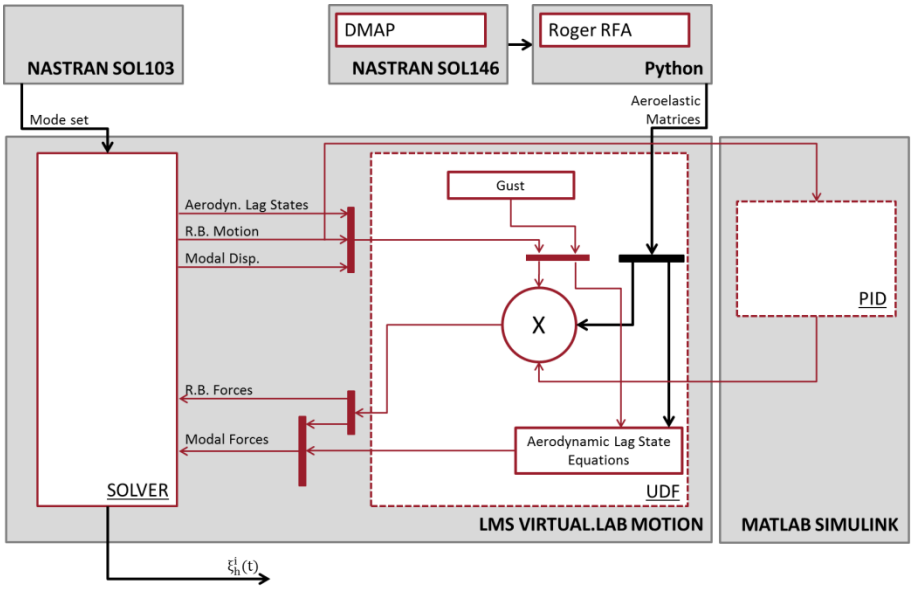

Figure 5. Multibody Aeroservoelastic Solution Environment

VI.Numerical Results

A. Unsteady Aerodynamic Forces Implementation Validation

In this study, the aircraft was subjected to a discrete gust in the form of a '1-cosine' gust, such that the velocity profile acted in a vertical direction normal to the path of the aircraft.

Several aeroelastic analyses were made over a range of gust lengths for a given flight configuration: with reference to Eq. (9), w_{ref} was varied linearly from 13.4 m/s EAS at 15,000 ft to 7.9 m/s EAS at 50,000 ft, based on the FAA Federal Aviation Regulations. At the investigated flight altitude of 25,000 ft and Mach number of M=0.6, the gust reference velocity was 11.48 m/s EAS, while the gust lengths varied between 18 m and 214 m.

Figure 6 shows the aeroelastic model used for the analyses[39], given by a representative civil jet aircraft, whose structure was modelled using a "stick" model with lumped masses, and the aerodynamic forces determined using the doublet lattice panel method.

In Fig. 7 is showed the portion of structure of interest for the evaluation of the internal loads, it is also reported the local reference system respect to which the internal loads are expressed.

Figure 8 shows the time histories of the aircraft model in terms of wing-tip displacement and wing root bending over a set of gust lengths (18 m, 127 m, 214 m) in order to excite the system for different frequency ranges; a comparison is done by using a quasi-steady aerodynamic model, without lag aerodynamic effects, and a fully unsteady formulation for the aerodynamic forces. The plots show a very good correspondence between the Virtual.Lab Motion and the

Nastran gust analyses both for the quasi-steady and the unsteady aerodynamic models. As expected taking into account of the dynamic and lag effects of the aerodynamic forces allows a more accurate modelling of system response; this improvements are particularly evident for the shorter gust length characterized by higher frequency content. For the quasi-steady aerodynamic formulation it emerges a higher response of the structure for all the investigated gust lengths that suggest an underestimation of the effects due to the aerodynamic damping.

In Fig. 8(e) can be noticed a slight gap between the displacements of the Nastran and the Virtual.Lab Motion model for the shorter gust length, this was due a small difference of the aircraft global angle of attack after the gust event of the order of E-02 degree that led to a small difference in the rigid body translation of the two models. This effect is completely negligible and does not affect the accuracy of the local deformation of the structure as suggested by the loads plots that exhibit a very good correlation between the two models.

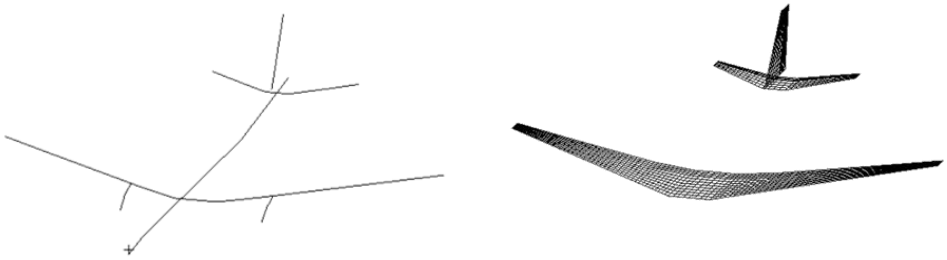

(a) Structural model (b) Aerodynamic model

Figure 6. Aeroelastic Model

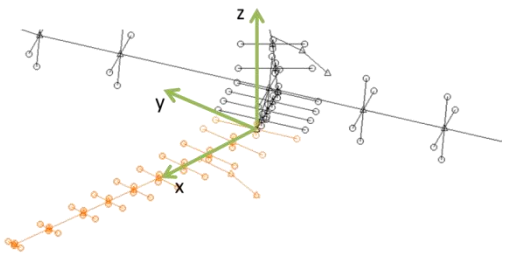

Figure 7.Structural Section and Reference System for the Loads Calculation

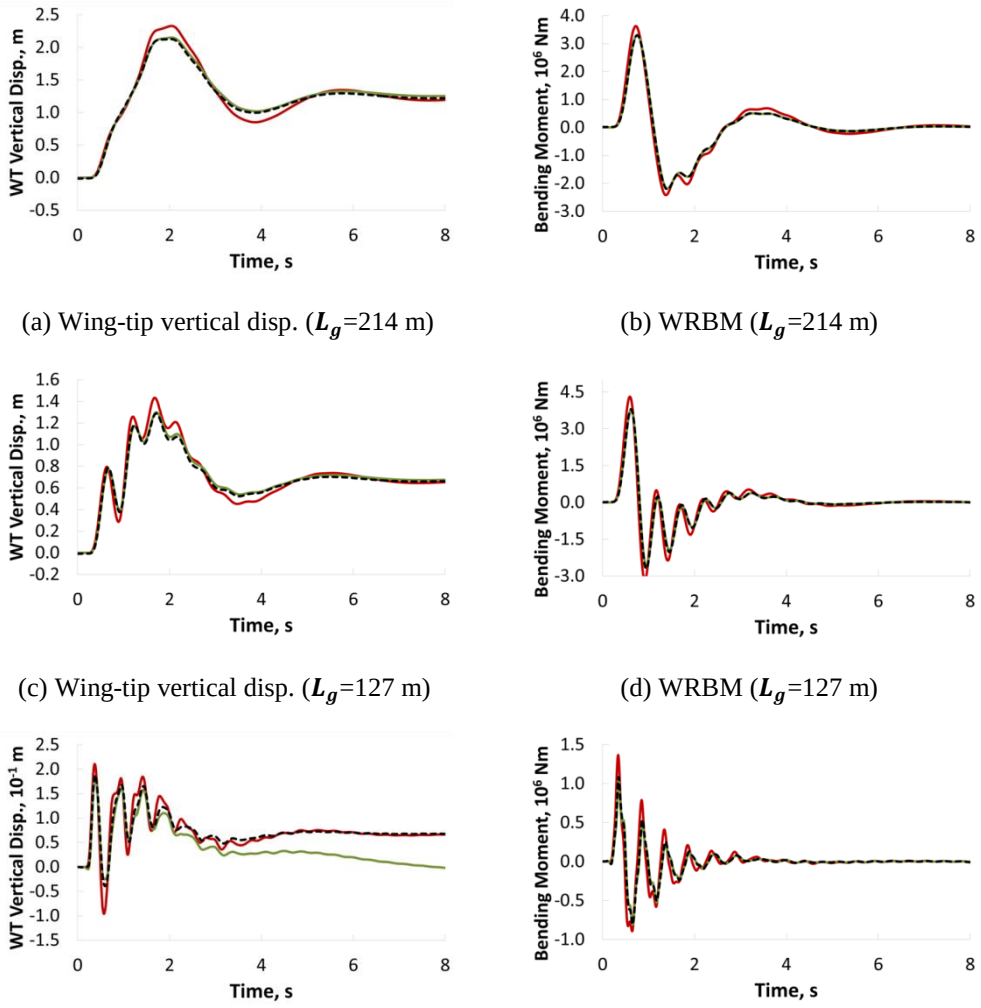

(a) Wing-tip vertical disp. (L_g=214 m) (b) WRBM (L_g=214 m)

(c) Wing-tip vertical disp. (L_g=127 m) (d) WRBM (L_g=127 m)

(e) Wing-tip vertical disp. (L_g=18 m) (f) WRBM (L_g=18 m)

Figure 8.Gust Response Analyses: Virtual.Lab Motion vs Nastran
(----: Nastran; ——: RFA (N_{Poles}=0); ——: RFA (N_{Poles}=5))

B. The Aeroelastic Landing Maneuver

The potentiality of including aeroelastic capabilities in multibody software can be fully exploited for the simulation of landing manoeuvres where it is essential to account for the combination of ground, aerodynamic and gust loads. The classic industrial approach, for the evaluation of landing loads, considers the aerodynamic loading as a constant load distribution which is determined in function of the initial condition (i.e. the flight condition before the touchdown). However the aerodynamic loads are not constant during landing manoeuvres therefore their evolution should be taken into account.

A significant effort has been done by previous authors[18-20]to implement aeroelastic loads in a landing manoeuvres. The proposed method consisted in the definition of a quasi-steady modal aerodynamic formulation using CFD data, unsteady aerodynamic effects were neglected.

In this Section an application of the implemented aeroelastic environment on landing manoeuvres is presented. Despite the limitations of the doublet lattice method in modelling the rigid body aerodynamic forces, as highlighted in previous section, this exercise still represents an interesting qualitative analysis showing the effects of lateral gust and landing loads combination, as reported in Fig. 9. A correction of the aerodynamics would be required for a quantitative evaluation of the aircraft loads.

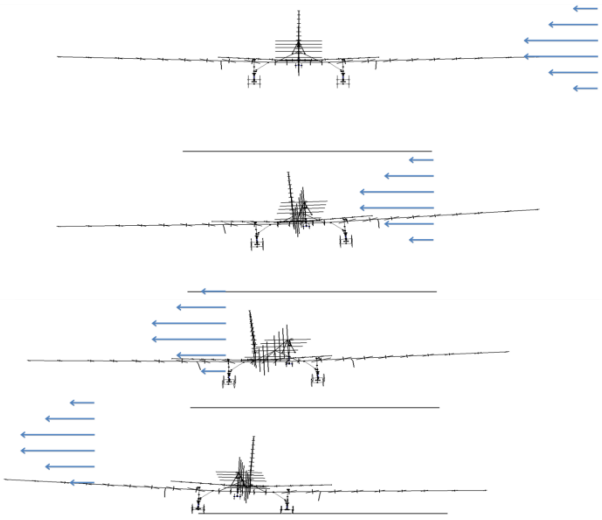

Figure 9. Landing Manoeuver with lateral wind shear

Two main landing gears and a nose landing gear were attached to a representative civil jet aircraft aeroelastic model[39]. A Craig-Bampton modal base, with flexible modes up to 30. Hz and static shapes for each rotational degree of freedom at the landing gear/airframe attachment nodes, was considered. The landing gear models have been produced by Siemens PLM ground loads experts, no modelling details were provided.

The model was assumed to operate at 0 ft of altitude with a Mach value of 0.2. The Flaps were also accounted as control surfaces with a 35° of deflection. Furthermore the dynamic pressure was evaluated in function of the actual longitudinal speed of the aircraft.

The analysis was performed in three different steps:

- Longitudinal trim analysis.

The trim of the aircraft motion was achieved by running in parallel the multibody code and Matlab Simulink. A constraint was defined at the aircraft centre of gravity leaving only the pitch degree of freedom and the forward motion as unconstrained. The vertical constraint force was measured and sent to Simulink. The trim was achieved through a PID control which modified the elevator deflection, and therefore the aircraft angle of attack, in order to set the vertical constraint force to zero. In such condition the lift would balance the aircraft weight, while the pitch moment equilibrium would be automatically satisfied being the model free to rotate to its neutral position. The elevator aerodynamic forces were evaluated and applied to the aircraft model through the UDF. A longitudinal speed of 75 m/s was defined as initial condition. A PID control was also used to define a longitudinal "thrust" force to be applied on the aircraft centre of gravity in order to keep the initial velocity constant by balancing the horizontal component of the lift due to the aircraft pitch motion since no aerodynamic drag was considered. This "thrust" is defined as a generalised force to be applied on the rigid body degrees of freedom only. Therefore it does not induce any deformation of the airframe since no generalized components are defined for the modal degrees of freedom. A more correct modelling would have required the thrust to be split in two components and then applied on the engine locations on order to account for the deformation effects induced on the wing. In the case considered in this work, the Authors have decided not to use this more sophisticated approach since the DLM aerodynamic model does not provide any drag component, therefore the deformation effects induced by the application of the thrust at the engine locations would have been overestimated. Figure 10 shows the results of the longitudinal trim analysis. Again a comparison with an equivalent Nastran model (with the landing gears modelled as lumped masses) shows a very good correlation of the trim results.

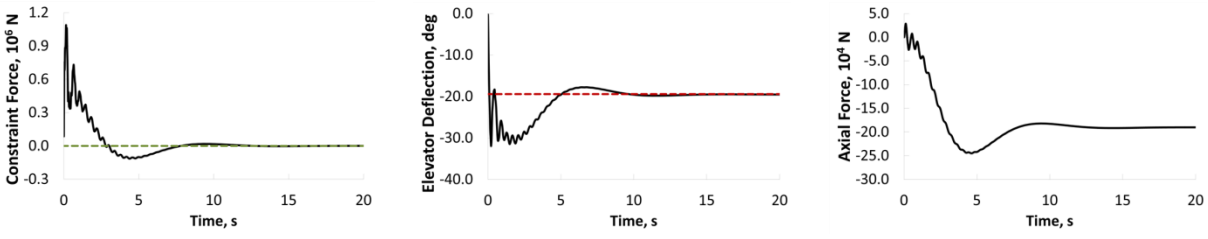

(a) Vertical constraint force (b) Elevator deflection (c) Longitudinal force

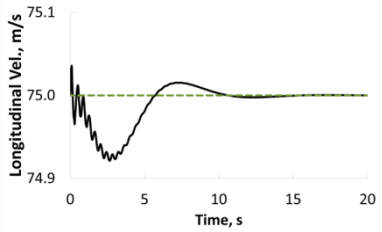

(d) Longitudinal velocity

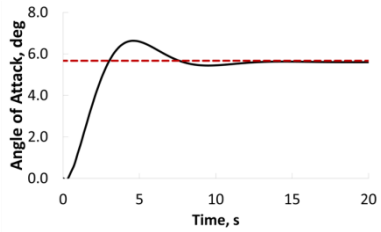

(f) Angle of attack

Figure 10. Aeroelastic Longitudinal Trim Results
(– – – –: Nastran; ——: VLM + Simulink; – – – –: target value)

- Steady descent trim analysis.

  Once the longitudinal trim was achieved the bracket on the aircraft centre of gravity was removed. A PID control was defined for the elevator and the axial force in order to modify the vertical speed from 0 m/s to -1.5 m/s following the profile in Fig. 11(a). The time variation of the trim variables are reported in Fig. 11.

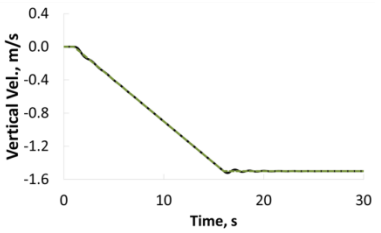

(a) Vertical velocity

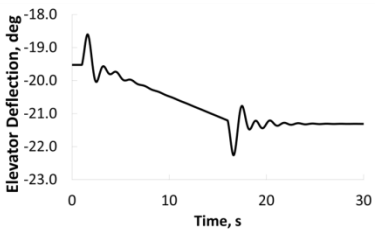

(b) Elevator deflection

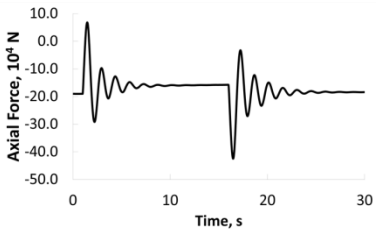

(c) Longitudinal force

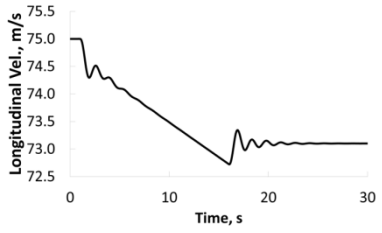

(d) Longitudinal velocity

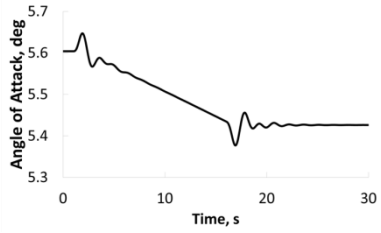

(f) Angle of attack

Figure 11. Aeroelastic Steady Descent Trim Results
(– – – –: Nastran; ——: VLM + Simulink; – – – –: target value)

- Touch down.

After the steady descent flight condition was reached, the axial forces and the elevator deflection were kept constant until the touchdown. Figure 12 reports the vertical and lateral tyre loads as well as the wing root vertical shear for a symmetric and an asymmetric landing due to a lateral gust. The results show how the lateral gust introduced significant variation on the aircraft structural loads. As expected a lateral component for the tyre forces was introduced. For the vertical tyre forces, a significant spike appeared around 17 s for the asymmetric case compared to the symmetric one. This was due to the fact that the aircraft touched the ground initially with one wheel, which, therefore, experienced very high loads level. The second spike, in common for the two landing cases, represents the nose landing gear touch down. For the internal structural loads a variation between the left and right wing root shear was observed for the asymmetric case.

The authors are aware that what is presented here is a pure qualitative application since all the aerodynamic nonlinearities (aircraft high lift configuration, ground effect, flow separation...) were neglected. A reliable flight mechanics model was missing as well. However the introduction of gust loads in a landing manoeuvre, still not present in the literature, provided a qualitative idea on how significantly the aircraft loads change when multidisciplinary load sources are combined. This represents, undoubtedly, an interesting starting point for this still immature research topic. The authors envisage the possibility of defining the recorded flight data as input for the UDF in order to replicate an actual landing incident thus provide a powerful and reliable tool for the incident loads assessment. This would represent a reasonable compromise, in term of accuracy and computational effort, between the simplified models (few degrees or freedom models or analytical formulas[40]), and a fully coupled CDF-structure solution which are currently used in the aeronautical industry.

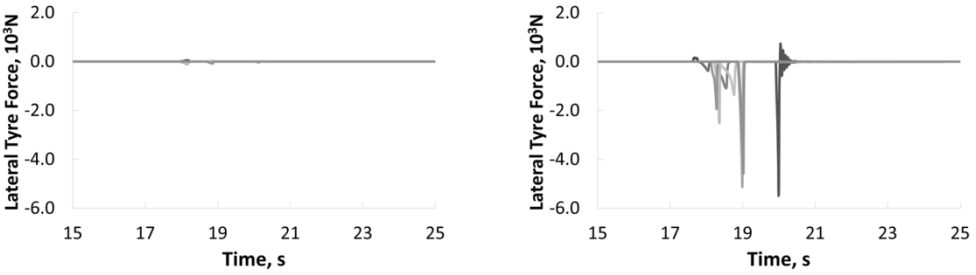

(a) Lateral tyre forces (symmetric landing) (b) Lateral tyre forces (asymmetric landing)

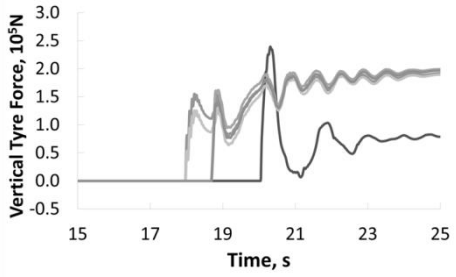

(c) Vertical tyre forces (symmetric landing)

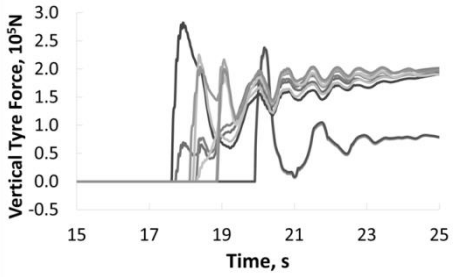

(d) Vertical tyre forces (asymmetric landing)

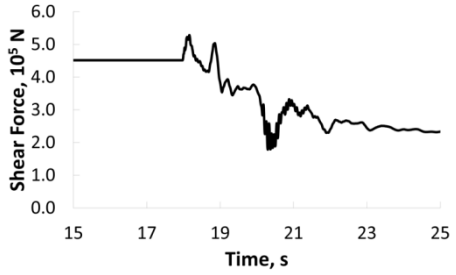

(e) Left and right wing root vertical shear (symmetric landing)

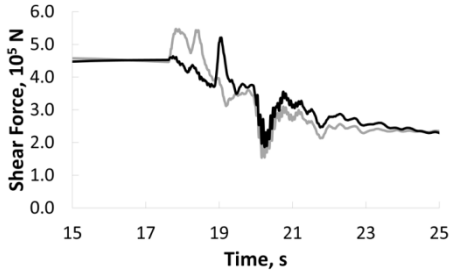

(f) Left and right wing root vertical shear (asymmetric landing)

Figure 12. Symmetric vs. Asymmetric Landing Loads

VII.Conclusions

A methodology to couple unsteady aerodynamic loads with flexible bodies in multibody simulations was presented. The implementation has been validated by comparing the trim results gust response of the Virtual.Lab Motion civil jet aircraft aeroelastic model with respect to an equivalent Nastran one.

An application was made in the simulation of a landing manoeuvre accounting for aeroelastic and gust loads showing a significant impact of the combined multidisciplinary loads sources over the aircraft loads evaluation.

It is concluded that, the implementation of an unsteady time domain formulation for the aerodynamics allows to use multibody simulation to accurate predict the aircraft aeroelastic loads with the same level of accuracy of the traditional FEM-based methods, but with remarkable advantage of allowing the simulations of other manoeuvres such as landings and the use of non-linear and active structures.

VIII. Acknowledgments

The research leading to these results has received funding from the European Community's Marie Curie Initial Training Network (ITN) on Aircraft Loads Prediction using Enhanced Simulation (ALPES) FP7-PEOPLE-ITN-GA-2013-607911 and also the Royal Academy of Engineering. The partners in the ALPES ITN are the University of Bristol, Siemens PLM Software and Airbus Operations Ltd.

References

[1] Albano E., Rodden W.P. (1969). "A Doublet-Lattice Method for Calculating Lift Distributions on Oscillating Surfaces in Subsonic Flows", AIAA Journal v7 n2 pp 279-285.

[2] Rodden W.P., Johnson E.H. (1994). "MSC/NASTRAN Aeroelastic Analysis' User's Guide", MSC Software.

[3] Looye G. (2005). "Integration of rigid and aeroelastic aircraft models using the residualised model method", In International Forum on Aeroelasticity and Structural Dynamics, number IF-046. CEAS/DLR/AIAAA.

[4] Rodden W.P., Love J.R., Equations of motion of a quasisteady flight vehicle utilizing restrained static aeroelastic characteristics Journal of Aircraft, 22(9), pp.802-809, 1985.

[5] Waszak M.R., Buttrill C.S., Schmidt D.K., Modeling and Model Simplification of Aeroelastic Vehicles: An Overview, NASA Technical Memorandum 107691, 1992.

[6] Meirovitch L., TuzcuI.Integrated Approach to the Dynamics and Control of Maneuvering Flexible Aircraft, NASA/CR-2003-211748, 2003.

[7] Meirovitch L., Tuzcu I., Unified theory for the dynamics and control of maneuvering flexible aircraft, AIAA journal, 42(4), pp.714-727, 2004.

[8] Kier T.M., Comparison of unsteady aerodynamic modelling methodologies with respect to flight loads analysis, AIAA Paper, 6027, p.2005, 2005.

[9] Reschke C., Looye G., Comparison of model integration approaches for flexible aircraft flight dynamics modelling, International Forum on Aeroelasticity and Structural Dynamics, number IF-046. CEAS/DLR/AIAAA, 2005.

[10] Patil M.J., Hodges D.H., Flight dynamics of highly flexible flying wings, Journal of Aircraft, 43(6), pp.1790-1799, 2006.

[11] Schütte A., Einarsson G., Raichle A., Schöning B., Mönnich W., Orlt M., Neumann J. Arnold J., Forkert T., Numerical simulation of maneuvering aircraft by aerodynamic, flight mechanics and structural mechanics coupling Journal of Aircraft, 46(1), pp.53-64, 2009.

[12] Ritter M., Dillinger J., Nonlinear numerical flight dynamics for the prediction of maneuver loads, International Forum on Aeroelasticity and Structural Dynamics, 2011.

[13] Kier T.M., Integrated Flexible Dynamic Maneuver Loads Models based on Aerodynamic Influence Coefficients of a 3D Panel Method, In 56th AIAA/ASCE/AHS/ASC Structures, Structural Dynamics, and Materials Conference (p. 0185), 2015.

[14] Lemmens Y., Verhoogen J., Naets F., Olbrechts T., Vandepitte D., Desmet W., Modelling Of Aerodynamic Loads On Flexible Bodies For Ground Loads Analysis, In International Forum on Aeroelasticity and Structural Dynamics, Bristol, 2013.

[15] Zhao Z., Ren G., Multibody dynamic approach of flight dynamics and nonlinear aeroelasticity of flexible aircraft, AIAA journal, 49(1), pp.41-54, 2011.

[16] Krüger, W.R. and Spieck, M., 2006. A multibody approach for modelling of the manoeuvring aeroelastic aircraft during pre-design. In Proceedings of the ICAS.

[17] Krüger, W., Multibody dynamics for the coupling of aeroelasticity and flight mechanics of highly flexible structures, Proceedings IFASD 2007.

[18] Spieck, M., Simulation of aircraft landing impact under consideration of aerodynamic forces on the flexible structure, In 10th AIAA/ISSMO Multidisciplinary Analysis and Optimization conference (Vol. 30), 2004.

[19] Krüger W.R., Spieck, M., Aeroelastic effects in multibody dynamics, Vehicle System Dynamics, 41(5), pp.383-399, 2004.

[20] Spieck M., Krüger W., Arnold J., Multibody simulation of the free-flying elastic aircraft, In Proceedings of 46th AIA/ASME/ASCE/AHS/ASC Structures, Structural Dynamics and Materials Conference. Austin, TX: AIAA., April 2005.

[21] Yue T., Wang L., Ai J., Multibody dynamic modeling and simulation of a tailless folding wing morphing aircraft, In AIAA Atmospheric Flight Mechanics Conference (p. 6155), August 2009

[22] Scarlett J.N., Canfield R.A., Sanders B., Multibody dynamic aeroelastic simulation of a folding wing aircraft, In Proceedings of the 47th AIAA/ASME/ASCE/AHS/ASC Structures, Structural Dynamics and Materials Conference, May 2006.

[23] Reich G.W., Bowman J.C., Sanders B.,FrankG.J.,Development of an integrated aeroelastic multibody morphing simulation tool, In Proceedings of the 47th AIAA/ASME/ASCE/AHS/ASC Structures, Structural Dynamics and Materials Conference, May 2006.

[24] Ameri N., Lowenberg M.H., Friswell M.I., Modelling the dynamic response of a morphing wing with active winglets, In AIAA Atmospheric Flight Mechanics Conference and Exhibit (pp. 1-19), August 2007.

[25] Cavagna L., Masarati P., Quaranta G., Simulation of maneuvering flexible aircraft by coupled multibody/CFD, Multibody Dynamic, 2009.

[26] Cavagna, L., Masarati, P. and Quaranta, G., Coupled multibody/computational fluid dynamics simulation of maneuvering flexible aircraft, Journal of Aircraft, 48(1), pp.92-106, 2011.

[27] Shabana A. (1989). "Dynamics of Multibody Systems", John Wiley Sons.

[28] Shabana A.A., Flexible multibody dynamics: review of past and recent developments, Multibody system dynamics 1.2: 189-222, 1997.

[29] Bampton, M.C.C., Craig, R.R. Jr., Coupling of substructures for dynamic analyses, AIAA Journal, Vol. 6, No. 7, pp. 1313-1319, 1968.

[30] Canavin J.R., Likins P.W. (1977). "Floating Reference Frames for Flexible Spacecraft", Journal of Spacecraft and Rockets, 14(12):724–732.

[31] Agrawal O.P. , Shabana A.A. (1986), Application Of Deformable-Body Mean Axis To Flexible Multibody System Dynamics, Computer Methods in Applied Mechanics and Engineering Vol. 56, Issue 2, pp.217-245.

[32] Wright J.R., Cooper J.E. (2007). "Introduction to Aircraft Aeroelasticity and Loads", John Wiley.

[33] Bisplinghoff R. L., Ashley H., Halfman R. L., Aeroelasticity, Dover, New York, 1996.

[34] Roger K.L. (1977). "Airplane Math Modeling Methods For Active Control Design", AGARD Structures and Materials Panel, A CP-228, pp 4-11.

[35] Mor M., Livne E., Sensitivities and approximations for aeroservoelastic shape optimization with gust response constraints, Journal of aircraft, 43(5), 1516-1527, 2006.

[36] Moulin B., Karpel M., Gust loads alleviation using special control surfaces, Journal of Aircraft, 44(1), 17-

25, 2007.

[37] Giesing J. P., Rodden W. P., Stahl B., Sears function and lifting surface theory for harmonic gust fields, Journal of Aircraft, 7(3), 252-255, 1970.

[38] Karpel M., Moulin B., Chen P. C., Dynamic response of aeroservoelastic systems togust excitation, Journal of Aircraft, 42(5), 1264-1272, 2005.

[39] Castrichini A.,HodigereSiddaramaiah. V., Calderon. D.E., Cooper J.E., Wilson T. & Lemmens Y. "Preliminary Investigation of Use of Flexible Folding Wing-Tips for Static and Dynamic Loads Alleviation", Aeronautical Journal -New Series- · November 2016, DOI: 10.1017/aer.2016.108.

[40] Lomax T.L., Structural Loads Analysis: Theory and Practice for Commercial Aircraft,AIAA, 1996